



©DREAMSTIME

Optic-Flow-Based Collision Avoidance

Applications Using a Hybrid MAV

BY WILLIAM E. GREEN AND PAUL Y. OH

Recent terrorist attacks on the United States have exposed the need for better surveillance and situational awareness technologies. Organizations created to address these needs are aggressively funding research in the use of micro air vehicles (MAVs) for homeland security missions. Such missions have been occurring in caves, tunnels, and urban areas. By mimicking flying insects, which navigate in these complex environments regularly, an optic flow collision avoidance system for MAVs was prototyped. However, there were certain instances (e.g., flying directly into a corner) where this system failed. To address this, a new MAV platform was prototyped, which enabled a quick transition from cruise flight into a hovering mode to avoid such a collision. The hybrid MAV offers the endurance superiority of a fixed-wing aircraft along with the hovering capabilities of a rotorcraft. This article details the applications and design of a hybrid MAV in conjunction with sensing and control techniques to perform autonomous hovering and collision avoidance. This is, to the best of our knowledge, the first documented success of hovering a fixed-wing MAV autonomously.

The Novel MAV Platform

More often, homeland security and disaster mitigation efforts have taken place in unforeseen environments, which include

caves, tunnels, forests, cities, and even inside urban structures. Performing various tasks such as surveillance, reconnaissance, bomb damage assessment, or search and rescue within an unfamiliar territory is dangerous and also requires a large, diverse task force. Unmanned robotic vehicles could assist in such missions by providing situational awareness without risking the lives of soldiers, first responders, or other personnel. Although ground-based robots have had many successes in search-and-rescue situations [6], they move slowly, have trouble traversing rugged terrain, and can still put the operator at risk. Alternatively, small unmanned aerial vehicles (UAVs) can provide soldiers and emergency-response personnel with an eye-in-the-sky perspective (Figure 1). On an even smaller scale, tiny, bird-sized aircraft or MAVs can be designed to fit in a backpack and can be rapidly deployed to provide around-the-corner or over-the-hill surveillance. Navigating in urban environments, however, remains a challenging problem for UAVs. In [7], promising results are shown for a rotorcraft equipped with a SICK laser scanner. Because lift decreases with platform size, carrying this type of sensor on MAVs is not feasible.

To design an MAV that can fly autonomously in and around buildings, inspiration came from looking at nature. Flying insects, such as honeybees and fruit flies, use optic flow to navigate in complex and dynamic environments [2], [9]. By mimicking insect behaviors, we were the first to demonstrate tasks such as collision avoidance and landing inside an urban

Digital Object Identifier 10.1109/MRA.2008.919023

structure [4]. More recently, optic flow has been used outdoors to avoid collisions with a tall building and to navigate through canyons [5]. Although using optic flow outdoors in rich texture areas seems promising, there are some limitations when using this technique as the only sensing modality inside buildings (e.g., flying directly at a wall with no texture). To address these sensor limitations, we prototyped a fixed-wing MAV that is capable of a quick transition into the hovering mode to avoid collisions directly in front of the aircraft. This article illustrates how integrating optic flow sensing, for lateral collision avoidance, with a novel MAV platform results in a vehicle that is well suited for flight in urban areas. The article also discusses optic flow and reactive control experiments mimicking flying insects as well as the fixed-wing MAV with hovering capabilities. The autonomous control of the aircraft's attitude during a hover is detailed later along with near-future goals.

Optic Flow

Insects perform tasks such as collision avoidance and landing by perceiving the optic flow of their surroundings. Optic flow refers to the apparent motion of texture in the visual field

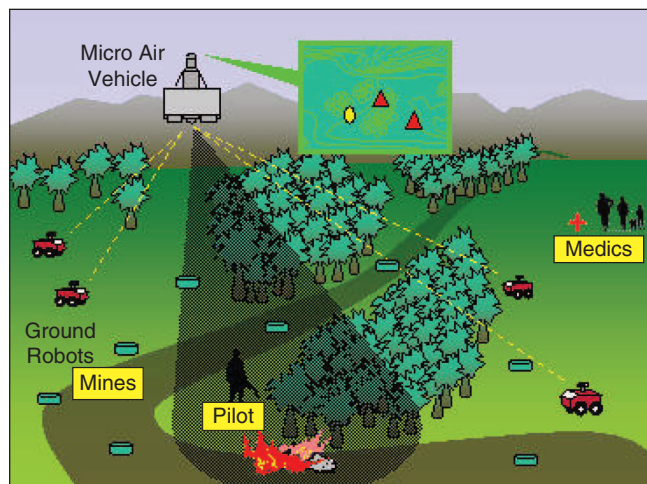


Figure 1. A small UAV is hovering above to acquire and distribute situational awareness to command and control personnel.

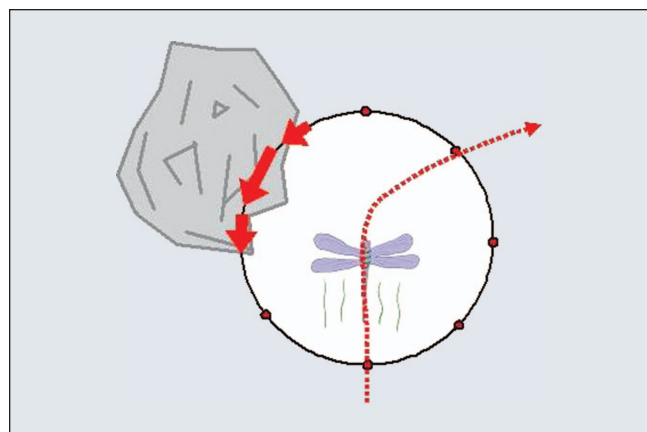


Figure 2. A dragonfly saccading away from regions of high optic flow to avoid a collision.

Insects perform tasks such as collision avoidance and landing by perceiving the optic flow of their surroundings.

relative to the insect's body. On the basis of several experiments with honeybees [8] and fruit flies [10], it is suggested that flying insects avoid collisions by turning away from regions of high optic flow (Figure 2). To mimic these navigation techniques, a 30-g flying testbed was prototyped. Figure 3 shows the prototype that was designed to be small and fly at 2 m/s for extended reaction times to avoid detected obstacles.

Collision Avoidance

Mimicking behaviors of flying insects required optic flow to be measured in front of the aircraft to detect oncoming collisions (Figure 4). Figure 5 shows a one-dimensional (1-D) optic flow sensor, developed by Centeye, that was used in the experiments. It comprises a mixed-mode vision chip that images the environment and performs low-level processing using analog very large scale integration (VLSI) circuitry [1].

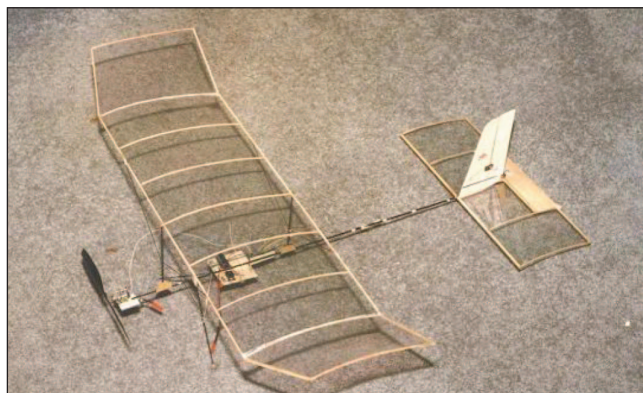


Figure 3. Our 30-g prototype with a 60-cm wingspan flies at speeds of 2 m/s.

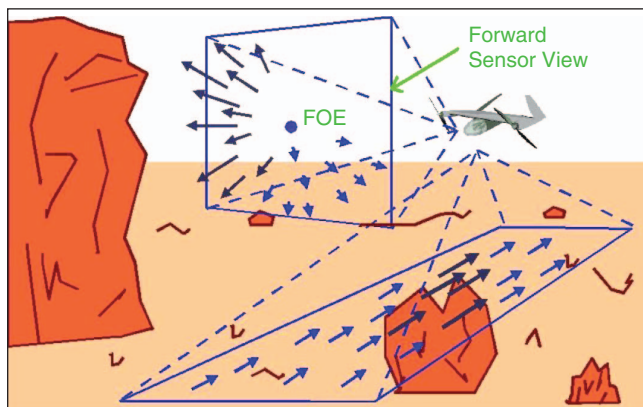


Figure 4. Optic flow as seen by an aerial robot flying above the ground.

Navigating in urban environments remains a challenging problem for UAVs.

Then, an off-the-shelf microcontroller performs mid- and high-level processing using standard digital techniques. The resulting sensor, including optics, imaging, processing, and input-output (I/O), weighs 4.8 g. This sensor grabs frames at up to 1.4 kHz and measures optic flow up to 20 rd/s.

Using two of these sensors angled at $\pm 45^\circ$ from the fuselage, optic flow fields were detected on each side of the aircraft. Optic flow is measured in rd/s and is a function of the MAV's forward velocity, V , angular velocity, ω , distance, from an object, D , and the angle, α , between the direction of travel and the sensor's optical axis (Figure 6). The formula, originally derived in [12],

$$OF = \frac{V}{D} \sin \alpha - \omega \quad (1)$$

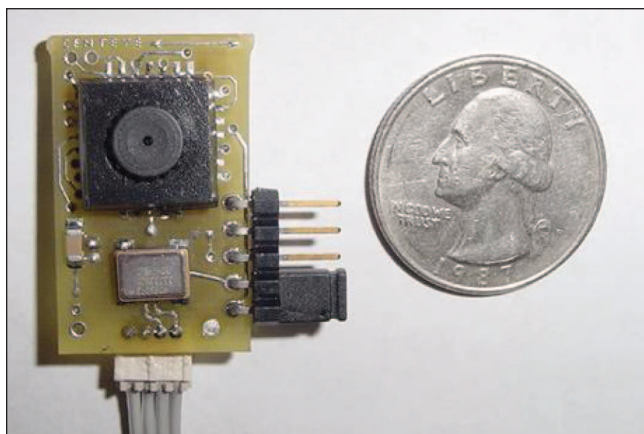


Figure 5. The mixed-mode VLSI optic flow microsensor is slightly bigger than a U.S. quarter.

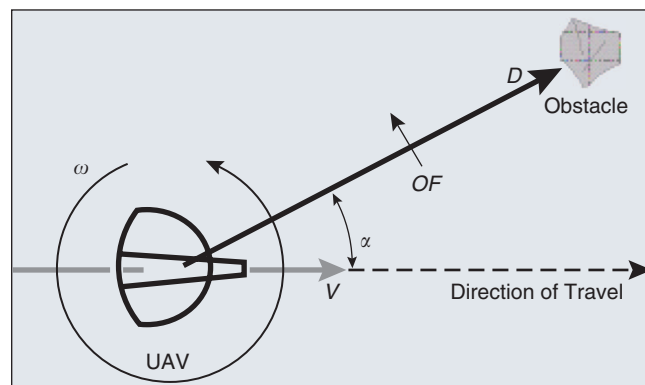


Figure 6. 1-D optic flow during the MAV's steady-level flight.



Figure 7. Optic flow is used to sense when an obstacle is within two turning radii of the aircraft. The aircraft avoids the collision by fully deflecting the rudder.

was used to set an optic flow threshold that corresponded to D being twice the turning radius of the aircraft. The threshold assumed cruise conditions (i.e., $V = \text{constant}$ and $\omega = 0$) and was preset experimentally.

The aircraft was then flown toward different obstacles, and an approaching object on either side of the MAV would generate an increase in optic flow as seen in (1). The output of each of these sensors was fed into an onboard microcontroller. If the values from either of the sensors exceeded the threshold, the processor would apply full deflection to the rudder to avoid the collision. By implementing this reactive-based method, autonomous collision avoidance was successfully demonstrated (Figure 7).

Optic Flow Limitations

The proof-of-concept experiments showed promising results for using optic flow for lateral collision avoidance. However, there are some limitations when flying directly toward an object. For example, when two optic flow sensors are aligned at 45° from the fuselage, as shown in the experiments discussed previously, smaller objects such as poles could remain outside the sensor's field of view [see Figure 8(a)]. This is most likely why honeybees never fly in a straight line toward a target but rather make a slight zigzag pattern. This generates an artificial parallax that will yield optic flow values for smaller oncoming obstacles.

Tiny, bird-sized aircrafts or MAVs can be designed to fit in a backpack.

Similarly, optic-flow-based collision avoidance is also insufficient when flying directly toward larger obstacles such as walls. Figure 8(b) shows an example of this scenario. In [14], the diverging optic flow field generated by the wall was used to trigger a warning 2 m before the collision. However, the experiment was performed in an artificially textured environment (i.e., alternating white and black sheets were used as walls). Realistically, walls are often homogeneous and have little texture. Therefore, this method will most likely fail, especially since the wall will be the only object in the sensor's field of view. When fruit flies are presented with this scenario in [11], they stick out their legs in preparation for landing. Landing on a wall is obviously not feasible for MAVs. However, a quick transition to a stationary attitude is possible; i.e., a fixed-wing MAV can be designed to quickly transition to a hover to avoid collisions in these instances.

Fixed-Wing Hovering MAV

Integrating the endurance of a fixed-wing aircraft with the hovering capabilities of a rotorcraft have recently been realized in the radio-controlled (RC) community through a maneuver known as prop-hang. During a prop-hang, the longitudinal axis of the fuselage is completely vertical, and the thrust from the motor balances the weight of the aircraft. Leveraging this maneuver, we were able to prototype a fixed-wing platform with an additional flight mode for hovering [3]. Figure 9 shows the prototype in its hovering attitude. The prototype is constructed with a 3-mm depron foam core laminated with

carbon fiber cloth. It has a 1-m wingspan, weighs 600 g, and could fly in cruise mode for 30 min on a 11.1-V, 1,320-mAh lithium polymer battery. With a 6.6:1 gear ratio and a brushless motor, which yielded 900 g of thrust, the MAV has a thrust-to-weight (T/W) ratio of 1.5. This high T/W ratio was required to balance the weight of the aircraft and an extra 100-g payload when in hover mode. In cruise flight (i.e., wings parallel to the ground), it has a speed range of 5–20 m/s.

Transition Between Flight Modes

The most critical aspect of the hybrid design is the transition from cruise to hover flight, which will be used as a secondary collision avoidance maneuver (Figure 10). During this phase,

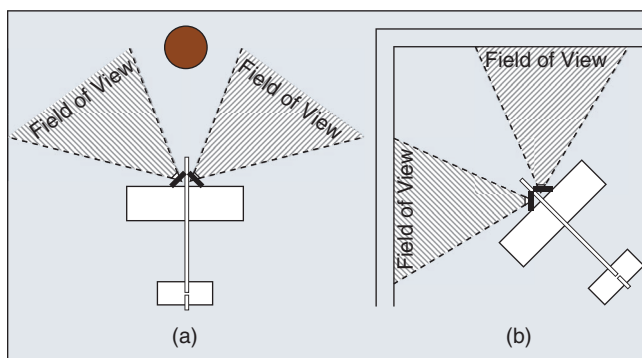


Figure 8. Limitations of using optic flow for navigation.

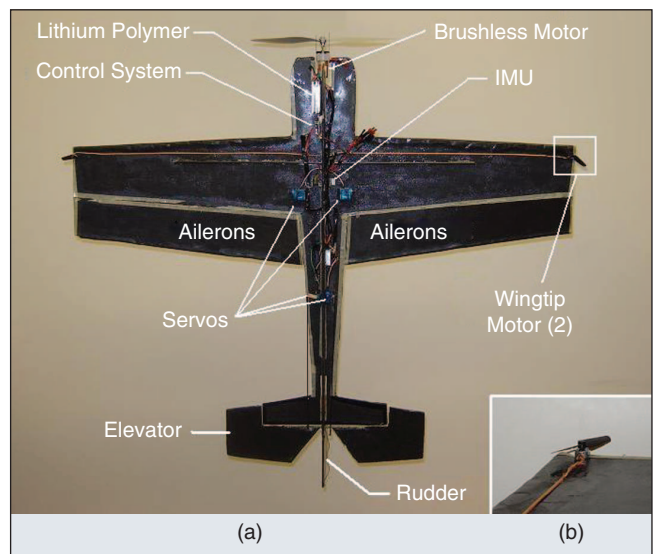


Figure 9. (a) Our hybrid prototype. (b) The wingtip motors are added to counter the rotation about the roll axis during a hover (i.e., torque roll).

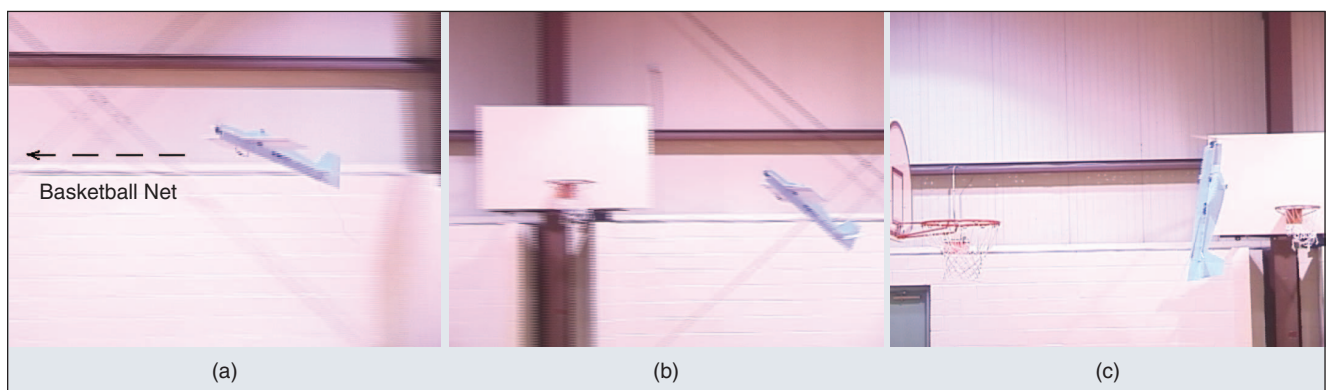


Figure 10. Our MAV prototype with a 1-m wingspan manually transitions from (a) cruise flight through (b) the stall regime and into (c) a hovering position to avoid collision with a basketball net.

Flying in and around caves, tunnels, and buildings demands more than one sensing modality.

there exists an angle-of-attack, α , for which the wings are no longer a contributing factor to the lift component (i.e., stall). To achieve the transition, the aircraft has to leverage its momentum and essentially overpower its way through the stall regime. This requires a high T/W ratio so that the momentum is not lost through the transition. Furthermore, as the aircraft is transitioning from cruise flight (minimum thrust) to the hovering flight mode, the throttle must be increased to balance the weight of the aircraft. The transition back to cruise mode is less complex. Vertical acceleration is required first to give the plane

some momentum, and then the elevator is deflected to pitch the aircraft forward into cruise mode.

Hovering

After transitioning into the hovering mode, the attitude must be sustained by constantly adjusting four channels of an RC transmitter (Figure 11). Assuming the aircraft is in or close to the hovering attitude (i.e., fuselage is vertical), an expert human pilot must ensure the following: 1) increase or decrease the throttle if the plane begins to lose or gain altitude, 2) apply left or right rudder deflection if the plane begins to yaw to the left or right, 3) administer the up or down elevator if the aircraft starts to pitch forward or backward from the nose-up position, and 4) counter the moment created by the motor torque by deflecting the ailerons. Steps 1–3 are shown in more detail in Figure 12, which shows the forces acting on the MAV during a hover. The forces generated by the rudder and elevator deflection angles regulate the aircraft's attitude, while the thrust force balances the aircraft weight. Summing the forces in the vertical direction yields

$$(T - D - F_E \sin \delta_E - F_R \sin \delta_R) \cos \psi \cos (\theta - 90) - W = ma_z, \quad (2)$$

where F_E and F_R are the elevator and rudder restoring forces, respectively, and are functions of the drag force, D , and control surface deflection angle, δ . When the aircraft is in a perfect hover (i.e., $\theta = 90$, $\psi = \delta_E = \delta_R = a_z = 0$), the thrust must equal both the weight and drag forces.

Autonomous Hovering

To autonomously avoid a collision by transitioning into the hover mode, both the transition into hover and the hover itself must be automated. To regulate the attitude during a hover, data from a small and lightweight inertial measurement unit (IMU) are fed into an onboard control system. These data are captured during both manual and autonomous hovering and are used to compare the controller performance with that of an expert human pilot.

Sensing and Control

Autonomous attitude control of this aircraft requires a sensor that can measure the vehicle's orientation when pitch angles approach and exceed $\pm 90^\circ$. Figure 13 shows an IMU by MicroStrain that outputs a gyroscopically stabilized four-component quaternion describing the MAV's orientation with respect to the fixed earth coordinate frame. It weighs just 30 g (out of its protective casing) and is composed of three triaxial accelerometers and angular rate gyros as well as three orthogonal magnetometers. The IMU, using RS232 communications, will transmit orientation data to the host computer at a clock cycle of around 10 ms. Therefore, embedding the sensor on the MAV platform will enable an onboard microcontroller to obtain the aircraft's orientation at a rate of 100 Hz.

An onboard control system was designed using a PIC16F87 microcontroller and an RS232 converter chip to communicate serially with the IMU. The microcontroller pings the IMU for the measured quaternion, q_m , which corresponds to the MAV's

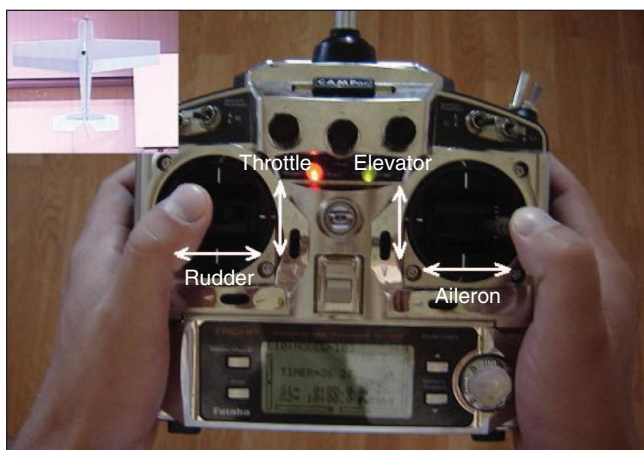


Figure 11. Manual hovering demands the control of all four transmitter channels.

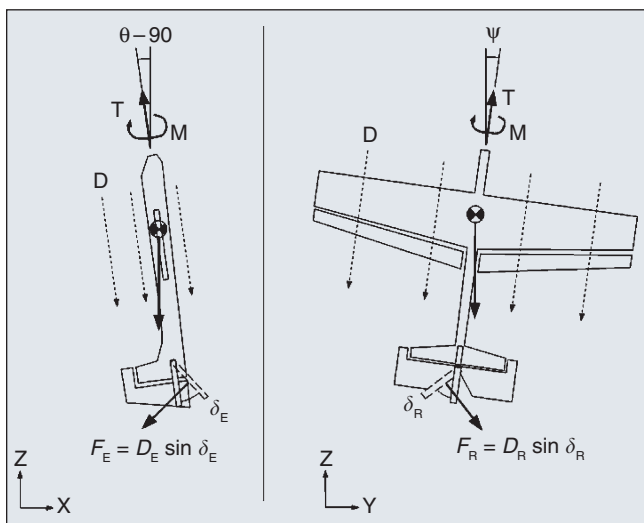


Figure 12. When in a hovering attitude, the elevator and rudder control surfaces are used to regulate the pitch and yaw angles, respectively.

attitude at that instant. The commanded quaternion, q_c , which describes the MAV's orientation during a hover, is

$$q_{1c} = e_1 \sin(\Theta/2) = 0.000i \quad (3)$$

$$q_{2c} = e_2 \sin(\Theta/2) = 0.707j \quad (4)$$

$$q_{3c} = e_3 \sin(\Theta/2) = 0.000k \quad (5)$$

$$q_{4c} = \cos(\Theta/2) = 0.707, \quad (6)$$

where e_i (for $i = 1, 2, 3$) represents the direction cosines of the Euler axis and Θ gives the scalar angle of rotation about that axis. The error quaternion can be found using the following formula [13]:

$$q_e = q_c^* \times q_m, \quad (7)$$

where q_c^* represents the conjugate of the commanded quaternion. The yaw and pitch error can be extracted from q_e , and the proportional-derivative control is used to send pulse-width modulated signals to the rudder and elevator servos. This, in turn, drives the aircraft orientation back to the hovering attitude. Figure 14 shows the control loop that repeats continuously and is synchronized with the IMU clock cycle (i.e., every 10 ms).

Experiments

The first autonomous hovering experiments were conducted inside an urban structure with limited flying space (i.e., 3×3 m area) to demonstrate that hovering can be sustained within small areas. The MAV's attitude is under full autonomous control through rudder and elevator inputs, while the height is adjusted manually through throttle commands via the pilot until the aircraft's weight is balanced. Initial experiments demonstrated that the MAV was able to successfully hover in hands-off mode for several minutes before draining the battery (Figure 15).

Another experiment was performed to contrast hovering under both manual and autonomous control. The metrics used were the duration of the hover before losing control and the stability of the aircraft while in the hovering mode. A skilled human pilot was initially given control of the aircraft and was instructed to fly around a gymnasium in cruise configuration, then transition from cruise to hover flight and attempt to hover the aircraft for as long as possible. The video stills in Figure 16(a)–(c) show the pilot struggling to keep the fuselage vertical but able to keep the aircraft positioned over a small area. (The video sequence shows three images extracted once

The hybrid MAV offers the endurance superiority of a fixed-winged aircraft along with the hovering capabilities of a rotorcraft.

per second for a period of 3 s. With the plane rotating at a rate of 0.25 r/s, this is enough to show two quarter rotations.) After a few trials, the human pilot was able to sustain a hover for several minutes before draining the battery. However, the aircraft's pitch and yaw angles oscillated significantly as the pilot tried to maintain the hover. This is supported with a portion of the captured flight data, labeled human-controlled, in Figure 17. Next, the pilot was instructed to again fly in cruise configuration and manually transition from cruise to hover flight. However, instead of trying to hover the aircraft manually, the pilot flicked a switch on the transmitter, which

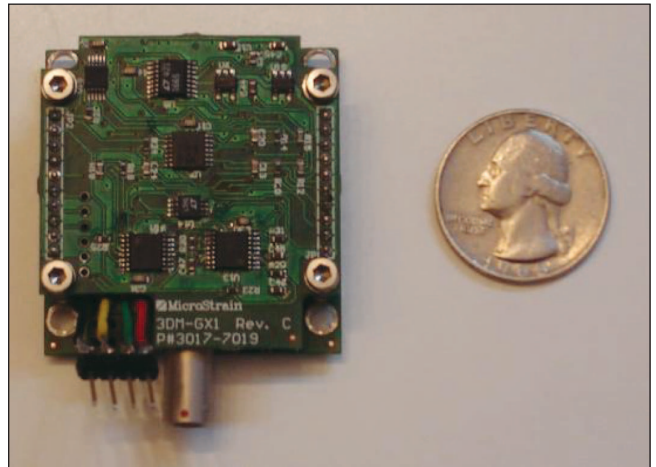


Figure 13. MicroStrain's 30-g IMU sensor was used to obtain attitude information on the onboard control system.

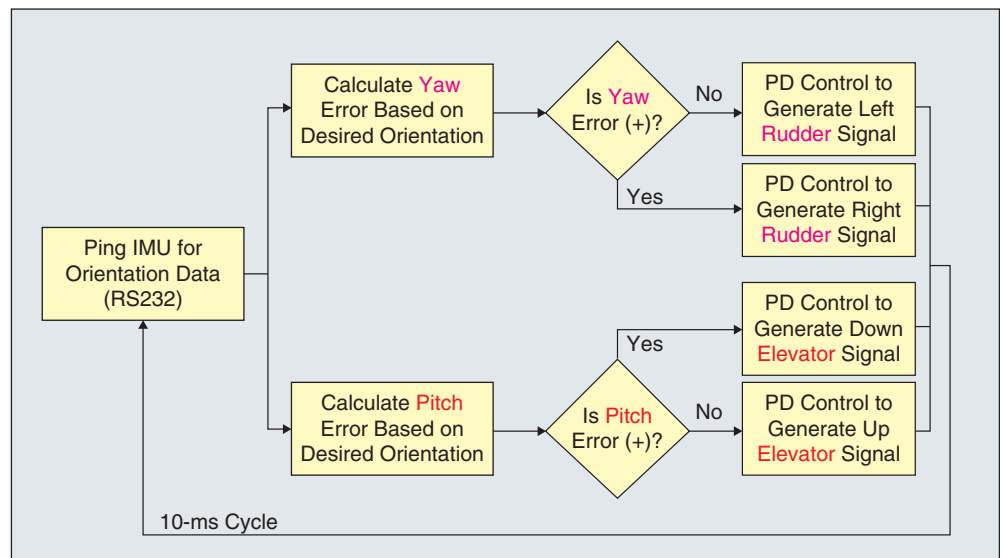


Figure 14. Flow chart describing the autonomous hovering code.

enabled the onboard control system. This time, the aircraft was fixed in a vertical position and was able to hover for more than 5 min before exhausting the battery [see Figure 16(d)–(f)]. Again, flight data were captured and a fraction of it is shown in Figure 17.

As originally thought, the torque-roll did not affect the stability of the aircraft during a hover; i.e., the MAV was still able to remain in the vertical position despite the rotations resulting from the motor torque. However, if this MAV were to be used in the field for surveillance and reconnaissance purposes, the view from the wireless camera onboard would have a dizzying effect as the plane was rotating at a rate of 15 r/min.



Figure 15. (a) A photograph from the MAV's bellycam is shown. (b) MAV performing a hands-off autonomous hover in an urban structure.

As the original aileron surface area did not create enough torque to counter the rotation, other alternatives had to be investigated. The first and most obvious was to increase the aileron surface area by lengthening them in the direction of the wing chord. However, this did not work because 1) the prop wash during a hover only flowed over about 30% of the aileron and 2) a longer aileron when fully extended caused some airflow to completely miss the tail, which greatly affected attitude regulation during a hover. The second approach was to mount miniature dc motors on each wingtip, which blow in opposite directions to create a rotational force opposite that of the motor torque (see Figure 9). Original experiments showed promising results as the torque rolling rate was decreased by more than 75%. Slightly more powerful motors are currently being investigated.

Conclusions

Flying in and around caves, tunnels, and buildings demands more than one sensing modality. This article presented an optic-flow-based approach inspired by flying insects for avoiding lateral collisions. However, there were a few real-world scenarios in which optic flow sensing failed. This occurred when obstacles on approach were directly in front of the aircraft. Here, a simple sonar or infrared sensor can be used to trigger a quick transition into the hovering mode to avoid the otherwise fatal collision. Toward this end, we have demonstrated a fixed-wing prototype capable of manually transitioning from conventional cruise flight into the hovering mode. The prototype was then equipped with an IMU and a flight control system to automate the hovering process. The next step in this research is to automate the transition from cruise to hover flight.

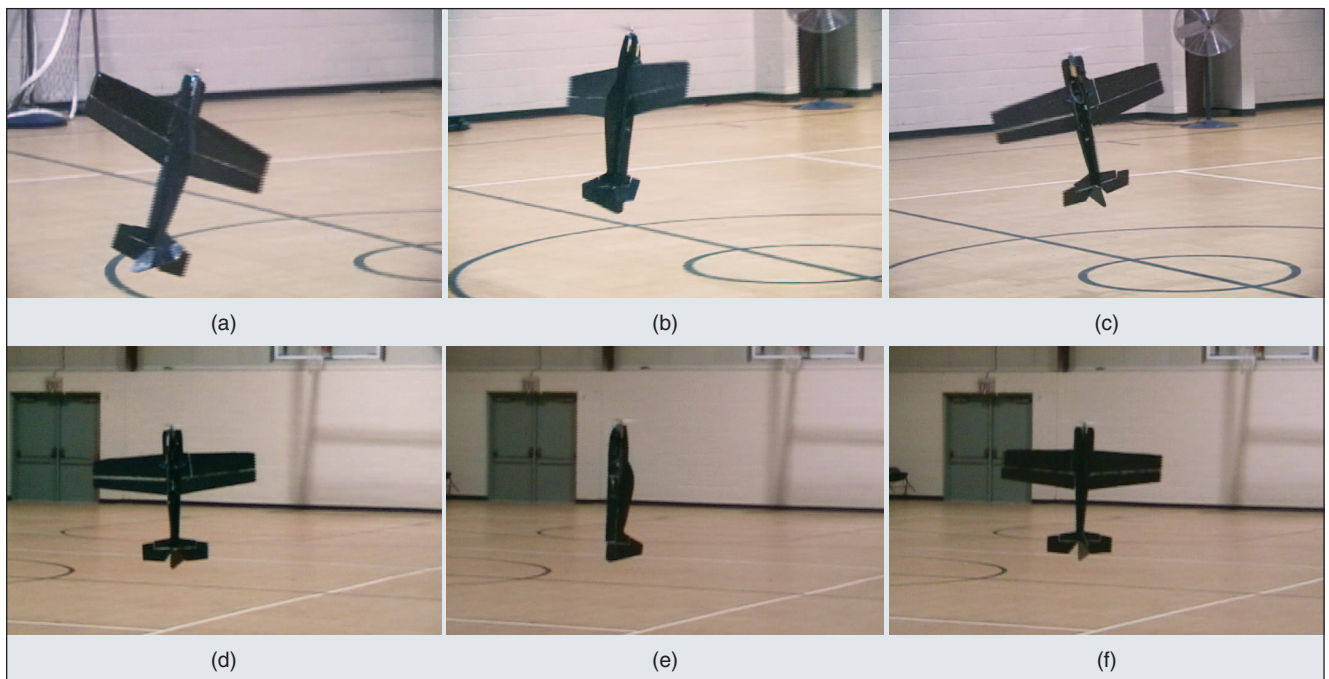


Figure 16. (a)–(c) A skilled-human pilot hovers a fixed-wing aircraft in a small gymnasium and struggles to maintain a vertical orientation. (d)–(f) Under autonomous control, the same aircraft is able to sustain a hover while remaining fixed in the vertical position.

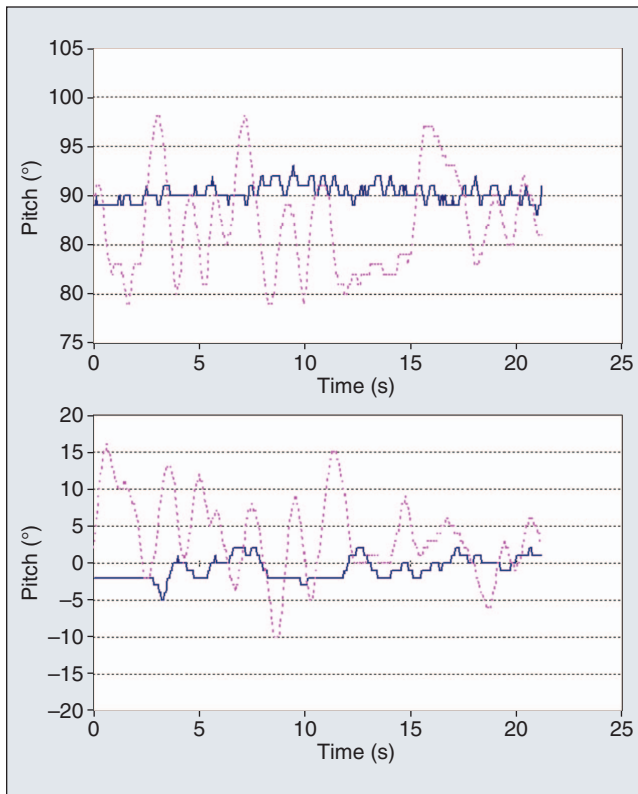


Figure 17. Pitch and yaw angles captured during both human-controlled and autonomous hovering.

Acknowledgments

This study is based on the work supported by the National Science Foundation under Grant No. 0347430. Any opinions, findings, conclusions, or recommendations expressed in this study are those of the author(s) and do not necessarily reflect the views of the National Science Foundation.

Keywords

Unmanned aerial vehicles, collision avoidance, hovering aircraft, autonomous, flight control.

References

- [1] G. Barrows, "Mixed-mode VLSI optic flow sensors for micro air vehicles," Ph.D. dissertation, Dept. Elect. Eng., Univ. Maryland, College Park, Dec. 1999.
- [2] J. J. Gibson, *The Ecological Approach to Visual Perception*. Boston, MA: Houghton Mifflin, 1950.
- [3] W. E. Green and P. Y. Oh, "An MAV that flies like an airplane and hovers like a helicopter," in *Proc. IEEE/RIS Int. Conf. Advanced Intelligent Mechatronics*, Monterey, CA, July 2005, pp. 699–704.
- [4] W. E. Green, P. Y. Oh, and G. Barrows, "Flying insect inspired vision for autonomous aerial robot maneuvers in near-earth environments," in

Proc. IEEE Int. Conf. Robotics and Automation, New Orleans, LA, Apr. 2004, pp. 2347–2352.

- [5] S. Griffiths, J. Saunders, A. Curtis, B. Barber, T. McLain, and R. Beard, "Maximizing miniature aerial vehicles," *IEEE Robot. Automat. Mag.*, vol. 13, no. 3, pp. 34–43, 2006.
- [6] R. Murphy, J. Casper, J. Hyams, M. Micire, and B. Minten, "Mobility and sensing demands in USAR," in *Proc. IEEE Industrial Electronics Conf. (IECON)*, 2000, vol. 1, pp. 138–142.
- [7] D. H. Shim, H. Chung, and S. S. Sastry, "Conflict-free navigation in unknown urban environments," *IEEE Robot. Automat. Mag.*, vol. 13, no. 3, pp. 27–33, Sept. 2006.
- [8] M. V. Srinivasan, S. W. Zhang, M. Lehrer, and T. S. Collett, "Honeybee navigation en route to the goal: Visual flight control and odometry," *J. Exp. Biol.*, vol. 199, no. 1, pp. 237–243, 1996.
- [9] M. V. Srinivasan, J. S. Chahl, K. Weber, S. Venkatesh, M. G. Nagle, and S. W. Zhang, "Robot navigation inspired by principles of insect vision," *Robot. Auton. Syst.*, vol. 26, no. 2, pp. 203–216, 1999.
- [10] L. F. Tammero and M. H. Dickinson, "The influence of visual landscape on the free flight behavior of the fruit fly *Drosophila melanogaster*," *J. Exp. Biol.*, vol. 205, pp. 327–343, 2002.
- [11] L. F. Tammero and M. H. Dickinson, "Collision avoidance and landing responses are mediated by separate pathways in the fruit fly, *Drosophila melanogaster*," *J. Exp. Biol.*, vol. 205, pp. 2785–2798, 2002.
- [12] T. C. Whiteside and G. D. Samuel, "Blur zone," *Nature*, vol. 225, pp. 94–95, 1970.
- [13] B. Wie, H. Weiss, and A. Arapostathis, "Quaternion feedback regulator for spacecraft eigenaxis rotations," *J. Guid. Control Dynam.*, vol. 12, no. 3, pp. 375–380, 1989.
- [14] J. C. Zufferey and D. Floreano, "Fly-inspired visual steering of an ultralight indoor aircraft," *IEEE Trans. Robot.*, vol. 22, no. 1, pp. 137–146, 2006.

William E. Green received his B.Sc., M.Sc., and Ph.D. degrees in mechanical engineering from Drexel University in 2002, 2004, and 2007, respectively. He is currently working with ATK in Maryland, USA.

Paul Y. Oh is an associate professor of mechanical engineering at Drexel University. He received his B.Eng. degree from McGill University in 1989. He received the M.Sc. degree from the Seoul National University in 1992 and his Ph.D. from Columbia University in 1999, both in mechanical engineering. He received faculty fellowships from the NASA Jet Propulsion Lab in 2002 and the Naval Research Lab in 2003. He received the NSF Career Award in 2004, the SAE Ralph Teetor Award for Engineering Education Excellence in 2005, and was named a Boeing Welliver Fellow in 2006. He is the director of the Drexel Autonomous Systems Lab, and he chairs the IEEE Technical Committee on Aerial Robotics.

Address for Correspondence: William E. Green, Drexel Autonomous Systems Laboratory, Drexel University, Philadelphia, USA. E-mail: william.edward.green@drexel.edu.